

BEAM SIZE MEASUREMENTS USING INTERFEROMETRY AT LHC

G. Trad*, E. Bravin, A. Goldblatt, S. Mazzoni, F. Roncarolo, CERN, Geneva, Switzerland
 T. Mitsuhashi, KEK, Ibaraki, Japan

Abstract

During the long LHC shutdown 2013-2014, both the LHC and its injector chain underwent significant upgrades. The most important changes concerned increasing the maximum LHC beam energy from 4 TeV to 6.5 TeV and reducing the transverse emittance of the beam from the LHC injectors. These upgrades pose challenges to the measurement of the transverse beam size via Synchrotron Radiation (SR) imaging, as the radiation parameters approach the diffraction limit. Optical SR interferometry, widely used in synchrotron light facilities, was considered as an alternative method to measure the 150 μm rms beam size at top energy as it allows measurements below the diffraction limit. A system based on this technique was therefore implemented in the LHC, for the first time on a proton machine. This paper describes the design of the LHC interferometer and its two SR sources (a superconducting undulator at low energy and a bending dipole at high energy), along with the expected performance in terms of beam size measurement as compared to the imaging system. The world’s first proton beam interferograms measured at the LHC will be shown and plans to make this an operational monitor will be presented.

INTRODUCTION

Measuring the transverse emittance of the beam is fundamental in every accelerator. This is particularly true for colliders, since the precise determination of the beam emittance is essential to maximize and control the luminosity. In the LHC, where it is not a directly accessible quantity, the emittance is inferred from the measurement of the transverse beam sizes and the knowledge of the accelerator optics. The LHC Beam Synchrotron Radiation Telescope (BSRT) is the only instrument offering non-invasive, continuous beam size monitoring via direct imaging of the emitted visible Synchrotron Radiation (SR). After the CERN long shutdown in 2013-2014, the maximum LHC beam energy was increased from 4 TeV to 6.5 TeV and the transverse emittance of the injected beam was reduced following upgrades in the injector chain upgrades. This makes the measurement of the transverse beam size via SR imaging a real challenge, as the radiation parameters approach the diffraction limit. Since the optical SR interferometer, widely used in synchrotron light facilities, allows beam size measurements below the diffraction limit, a system based on this technique was therefore implemented in the LHC, for the first time in a proton machine. In this paper, the design of the LHC interferometer is presented and its final version, installed in June 2016, is described. The characterization of its compo-

nents and the commissioning process with beam will also be discussed. Additionally the LHC beam size measurement via the world’s first measured proton beam interferograms will be shown and plans to make the interferometer an operational monitor will be presented.

LHC SR SOURCE

The LHC is equipped with two SR monitors (one per beam) used to characterise the transverse and longitudinal beam distributions. The SR source is a combination of a dedicated undulator and a beam separation dipole (D3). The visible SR emission point shifts gradually with the energy ramp from the undulator (at injection energy, 450 GeV) to the D3 which dominates from 1.2 TeV onwards [1]. The D3 is a 9.45 m long superconducting dipole and at 7 TeV, its maximum field is 3.9T giving a bending angle of 1.58 mrad and a radius of curvature of ~6 Km. The undulator was designed to enhance the visible SR component from injection energy up to ~1.2 TeV, until the contribution of visible SR from D3 becomes detectable. The undulator is installed 937 mm upstream of D3 and shares the same cryostat. It is made of two 28 cm periods with a peak field of 5 T, thus resulting in the undulator parameter “K” 0.0712. The emitted SR is intercepted by an extraction mirror installed in the beam vacuum and sent through a vacuum window to the BSRT. Figure 1 shows the SR intensity distribution on the extraction mirror, as simulated for injection and top energy.

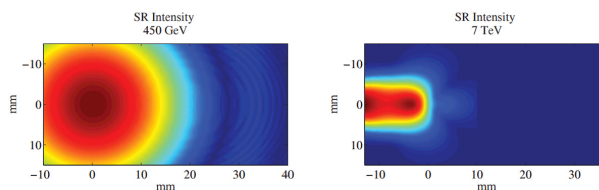


Figure 1: Simulated SR Intensity on the extraction mirror of the LHC at injection (left) and Flat Top (right).

SR IMAGING LIMITATION

The visible SR imaging system is based on two focusing stages, offering the possibility of switching between two different sets of lenses. One optimized for 400-600 nm operation at injection and the other for Near Ultra-Violet (NUV, 250 nm) imaging at high energy [2]. It is worth mentioning that the NUV operation was found beneficial in terms of resolution at high energy where the beam size is as small as 170 μm. In fact in LHC Run II, the BSRT resulted reliably operational for bunch-by-bunch measurements and crucial

* georges.trad@cern.ch

for several studies (beam-beam, instabilities and Electron Cloud studies). Crosschecks with independent emittance measurements, such as the luminosity scans, confirmed the accuracy of the BSRT beam size measurement to the level of 5%.

However, due the intrinsic limitation of the imaging system, originating from the error ϵ on the determination of the optical resolution σ_{LSF} that impacts the emittance ϵ_{Beam} determination [3], soon with the decreasing beam sizes, the SR imaging technique will be unsuitable for measurements.

INTERFEROMETRY

Direct imaging for beam size measurement is ultimately diffraction limited and very sensitive to the cross-calibration techniques. Interferometry is the best alternative to measure the small beam size with visible SR. It consists of determining the size of a spatially incoherent (or partially coherent) source by probing the spatial distribution of the degree of coherence after propagation, with a theoretically achievable resolution of a few microns. A rigorous derivation of the principle can be found in [4]. In the following only a brief summary of the technique is given.

Principle

The LHC interferometer is a wavefront-division-type two-beam SR interferometer using polarized, quasi-monochromatic light. The spatial coherence of the SR is probed by measuring the first order degree of mutual spatial coherence Γ .

The double slit samples the incoming wavefront to obtain the one-dimensional interference pattern along the vertical or horizontal axis. The intensity of the interference pattern measured on the detector plane is given by:

$$I(x) = I_0 \left[\text{sinc} \left(\frac{2\pi a}{\lambda_0 R} x \right) \right]^2 \cdot \left\{ 1 + |\Gamma| \cos \left(\frac{2\pi D}{\lambda_0 R} x + \phi \right) \right\} \quad (1)$$

with a the half of the single slit width, D the separation between the two slits, λ_0 the wavelength of observation, I_0 the sum of the incoherent intensities from both slits, ϕ an arbitrary phase and R the distance from the lens to the detector plane.

The visibility of the interferogram fringes, using the intensities I_{max} at the peak of the interference fringe and I_{min} at its valley, is defined as:

$$V = \frac{I_{max} - I_{min}}{I_{max} + I_{min}} = \frac{2\sqrt{I_1 \cdot I_2}}{I_1 + I_2} |\Gamma| \quad (2)$$

where I_1 and I_2 is the light passing through the first and the second slit respectively. The beam size is derived based on the Van Cittert-Zernike theorem [4], where the degree of coherence Γ is the Fourier transform of the intensity distribution of the source. The beam size can be obtained from the interferograms in the following two ways.

1-Fixed slit separation mode

This mode relies on the hypothesis of Gaussian beams. By acquiring and fitting the interference pattern to obtain the spatial coherence modulus $|\Gamma|$, the beam size σ_x is obtained using:

$$\sigma_x = \frac{\lambda_0 R_0}{\pi D} \sqrt{\frac{1}{2} \ln \frac{1}{|\Gamma|}} \quad (3)$$

with R_0 being the distance from the source to the double slits (for the LHC, 29.3 m at 450 GeV and 26.5 m at high energies).

2-Slit separation scanning mode

The intensity pattern is recorded for varying slit separation D and the beam shape $f(x)$ is obtained by applying an inverse Fourier transform of the resulting curve $\Gamma(D)$. Assuming Gaussian distributions:

$$\sigma_x = \frac{\lambda_0 R_0}{2\pi\sigma_v} \quad (4)$$

with σ_v being the RMS width of $|\Gamma|(D)$.

LHC INTERFEROMETER

After testing the prototype during the 2015 LHC run the final setup of the interferometer was installed in June 2016. It features a new slit assembly that allows the measurement of the horizontal and the vertical beam sizes with the possibility to change the slit width, separation, height and center remotely. The system can also be operated as a 2D interferometer by inserting at the same time the horizontal and vertical slits. The 2015 polarizer (seen to introduce additional focusing with strong astigmatism) was replaced with a high quality precision linear polarizer constructed by laminating a polymer polarizing film between two high-precision glass substrates (flatness better than $\lambda/6$). This was installed immediately at the entrance of the gated intensified sCMOS camera used to acquire the images. The overall magnification of the system was adapted to accommodate the full interferogram on the central region of the sensor.

COMMISSIONING AT 6.5TEV

The interferometer commissioning started in August 2016. A set of tests was carried out to check the functioning of all the 23 motorized component of the interferometer. The aim of these studies was to validate the light alignment, the focus, the magnification, the polarization and the slit configuration. To rule out the additional effects of the incoherent depth of field of the dipole SR, estimated to be dominant when measuring the horizontal beam size [5], this section will describe only a set of vertical beam size measurement via interferometry and how they compare to the imaging system.

Wavefront Distortion

One of the main concerns when designing an interferometer is the preservation of the SR wavefront from the extraction point up to the slits, since any distortion affects the beam size measurement. The quality of the in-vacuum

extraction mirror represents a major concern since it is exposed to heating by both SR and electro-magnetic coupling with the beam. Additionally, in order to reach the desired reflectivity over the whole visible SR spectrum, the coating process involves the deposition of multiple dielectric layers deposition. The resulting flatness is in the order of $\lambda/4$ peak to valley over the total mirror surface at ~ 600 nm. The extraction mirror deformations leads to an effective double slit separation. It depends on the mirror tilt, the distance from the source to the extraction mirror and on the distance from the mirror to the double slits. By design the latter was kept as small as possible such that the effects are minimized to $< \sim 2\%$ for all possible slit separations for typical mirror deformations. The mirror was as well checked using the installed "Hartmann Mask" line [6], that confirmed that no deterioration of its surface flatness is caused by the full intensity circulating beam [7].

Double Slit Height Dependence

When designing an interferometer, the slit height is normally chosen to cover the whole angular distribution of the SR radiation. However, when the SR is intense enough, restricting the slit height is beneficial for two reasons. Firstly, sampling small areas of the SR wavefront (i.e. using a smaller surface of the extraction mirror and successive optics) minimizes the waveform distortion and aberration effects. In addition, coupling effects between the horizontal and vertical beam size measurements that could become important when the two planes are very different [4] are minimized.

For LHC interferometer commissioning the SR intensity was enough even when reducing the slit height to $500 \mu\text{m}$. Despite the fact that no dependence of the measured beam size was observed for various slit heights all the following measurements, unless otherwise stated, use a slit height of $500 \mu\text{m}$.

Wavelength Dependence

The interferometer is equipped with two bandpass filters with a central wavelength of 400 and 560 nm, and width ± 10 nm. Although the lenses are optimized for 500 nm operation no big aberrations are expected for either wavelengths. Figure 2 shows the interferograms recorded for various slit separations with the fringe visibilities extracted for each separation using the 560 nm filter. Under the assumption of Gaussian beams, the fit of $V(D)$ gives a beam size of $375 \mu\text{m}$. A similar measurement with the 400 nm bandpass filter resulted in a beam size of $369 \mu\text{m}$. The two measurements are fully compatible and indicate that the measurements are practically immune to aberrations and tiny shifts in focus. This is confirmed by a set of simulations that estimate the error introduced by chromatic aberrations originating from the finite width of the bandpass filter to be $< 1\%$ for $\sigma_{Beam} > 200 \mu\text{m}$ [3].

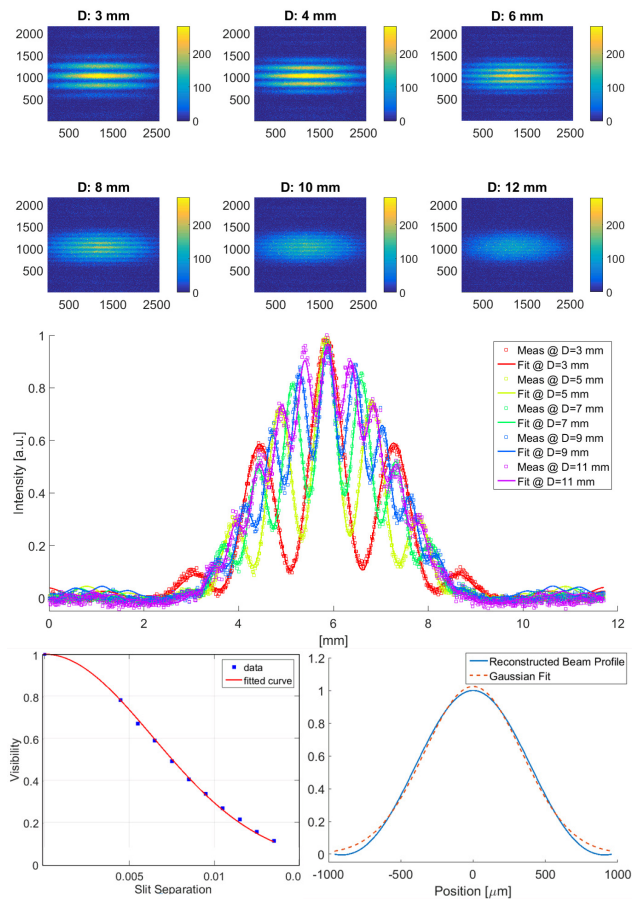


Figure 2: Interferogram recorded for various slit separation using the 560 nm filter. The projections are fitted using Eq. 1 and the inferred visibility is plotted against the slit separation and fitted with a Gaussian curve to extract the beam size by applying an inverse fourier to $|\Gamma(D)|$.

Frame Exposure Dependence

Beam oscillations and vibrations or air turbulence on the optical bench provoke a smearing of the interferogram visibility and a displacement of its centroid. The camera exposure was increased gradually from $200 \mu\text{s}$ to 200 ms in the interferograms presented in Fig. 3. Since the LHC revolution frequency is $\sim 89 \mu\text{s}$, this corresponds to integrating over 2 turns up to ~ 2000 turns. The measured beam size, 366 (MEAN) $\pm 5.6 \mu\text{m}$ (RMS), had very little dependence on the exposure time.

Intensifier Gain Dependence

The effect of image intensifier saturation on the recorded interferogram can be seen in Fig. 4 which shows the patterns recorded as the voltage applied to the image intensifier is changed from 0 to 2000 mV, and histograms of the pixel values. As long as the gain is kept lower than 900 mV the brighter pixels remain at values ≤ 1000 with the corresponding change of visibility resulting in an error on the beam size of $\leq 4\%$

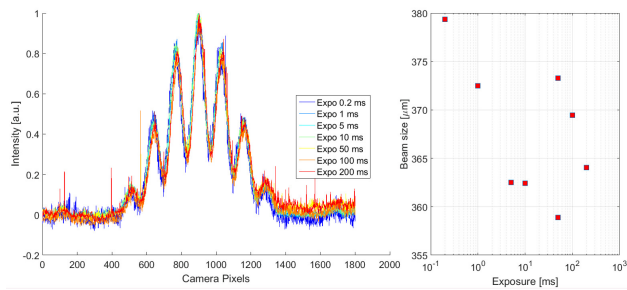


Figure 3: Left: interferograms at $\lambda=560$ nm and $D=6$ mm for various camera exposure times ranging from 200 μ s to 200 ms. Right: beam size extracted for each exposure.

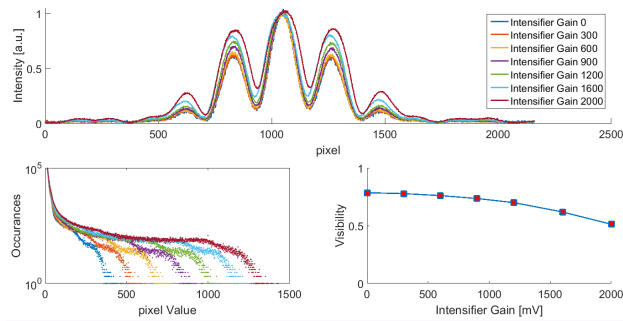


Figure 4: Upper plot, interferograms at $\lambda=560$ nm, $D=3$ mm recorded with various intensifier gains. Bottom left: histogram of pixel intensities. Bottom right: visibility curve as function of the intensifier gain.

Polarization Dependence

The horizontal and vertical polarizations of the SR lead to interference fringes shifted by π rad in phase [4]. When measuring both polarizations this results in a loss of the visibility (see Fig. 5) and an overestimation of the beam size. Since the polarizer is mounted on a motorized, rotating stage, a scan of the angle was carried out to identify the nominal position of the polarizer for selecting exclusively the H polarization (which is more intense than V).

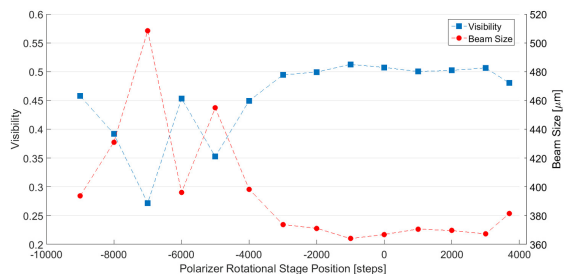


Figure 5: Visibility and the corresponding beam size for several positions of the polarizer rotational stage.

Double Slit Center Effect

If the double slit setup is not aligned with respect to the vertical fan opening of the SR, an intrinsic imbalance of the slit illumination is introduced. This contributes to an over-

estimation of the beam size even after applying the correction of Eq. 2. Such an effect can be interpreted as a consequence of the incoherent depth of field and the SR cone opening dependence on offsets in the bending plane [8]. Figure 6 clearly shows this effect when the center of the double slits was shifted by ± 8 mm from the nominal position. The error on the beam size measurements can be as high as 20 % when the slits are far from the medium plane, but remains within 5% when misaligned by ± 2 mm.

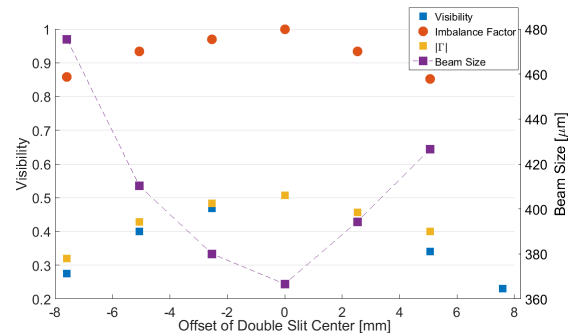


Figure 6: Intensity imbalance factor, fringes visibility before and after correction and the corresponding inferred beam size shown for various positions of the double slit center.

Detector Linearity

The interferogram visibility is strongly affected by the linearity of the detector (camera+intensifier), something which was tested in the laboratory. A broadband fiber lamp with very stable flux is used as a light source. A set of accurately calibrated neutral-density filters with optical density $\leq 0.1\%$ error in the 400 nm to 650 nm range [9] was used to vary the light input on the intensifier while images were recorded. The results are shown in Fig. 7. After subtracting the background image (with no light input) the detector shows a good uniformity ($< 1\%$ variation) and a good linearity with the maximum deviation from the linear fit $< 5\%$ (except for very low lighting conditions).

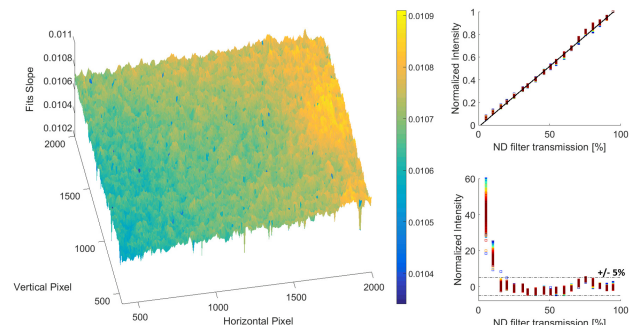


Figure 7: Detector uniformity and linearity as measured in the laboratory.

Benchmarking with the Imaging System

The beam size measured with interferometry was compared to the beam size measured via imaging in the BSRT.

The BSRT is operated in gated mode measuring bunch by bunch size, from which an average beam size is calculated. The beam size from imaging was always found smaller than the beam size from the interferometer by a factor of ~ 1.4 . The relative bunch by bunch size measured via interferometry (Fig. 8) was however found to be compatible with that observed through imaging.

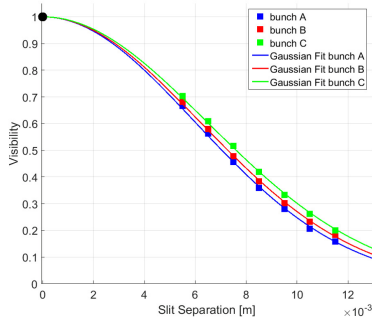


Figure 8: Visibility curve as function of slit separation for three different bunches with different sizes.

COMMISSIONING AT INJECTION ENERGY

Contrarily to Flat Top energy, the SR intensity emitted by the undulator at injection is low (3 orders of magnitude less). Since the beam size to be measured is also bigger (~ 1 mm), the visibility curve as function of the slit separation decays very rapidly and only small D values can be used. In order to obtain a useful interferogram to resolve the beam size, for a separation D in the order of 2.5 mm the suitable slit width should be around 0.5 mm. Unfortunately for slit widths < 1 mm even with the smallest achievable optical magnification the pattern is as big as the detector area and no reliable fits could be obtained since the background is hardly recognizable. Therefore for the measurements at 450 GeV the width is set to 1 mm. Figure 9, shows horizontal and vertical beam size measurement, for two different bunches with the minimum slit separation possible (2.4 mm and 2.6 mm for the horizontal and vertical planes respectively). The extracted beam sizes are summarized in Table 1. The results are found very much compatible with the imaging values and discrepancies are $\sim 5\%$.

Table 1: Horizontal and vertical beam size measurement at Injection for 2 different bunches via imaging and interferometry.

	σ [mm]	bunch 1		bunch 62	
		H	V	H	V
450 GeV	Imaging	1.22	1.6	1.15	1.4
	Interferometer	1.20	1.53	1.14	1.34

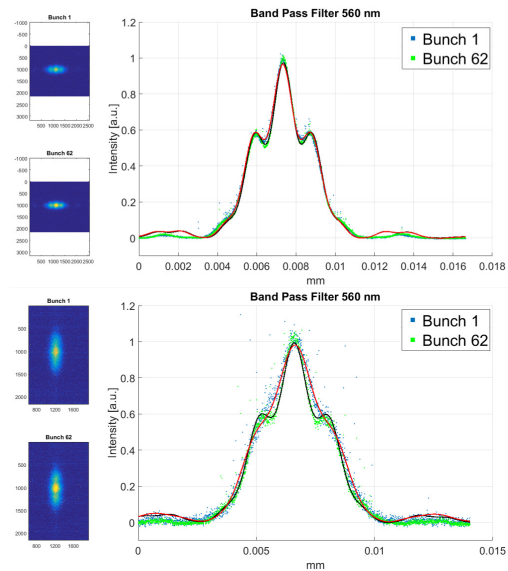


Figure 9: Top Plot: Interferogram with $D=2.4$ mm, $a=1.5$ mm for horizontal size measurement with 200 ms exposure at $\lambda=560$ nm. Bottom Plot: Interferogram with $D=2.6$ mm, $a=1$ mm for vertical size measurement with 200 ms exposure at $\lambda=560$ nm.

2D INTERFEROMETER

The interferometry setup also allows the simultaneous measurement of the horizontal and vertical beam size. Two dimensional interferograms are obtained by arranging the motors to obtain four small slits distributed along the corners of a rectangle whose sides D_H and D_V represent the slit separation for the horizontal and vertical planes respectively. The results of a set of measurements in this configuration, for different slit separations, as well as a comparison to separate 1D scans are shown in Fig. 10. The excellent agreement

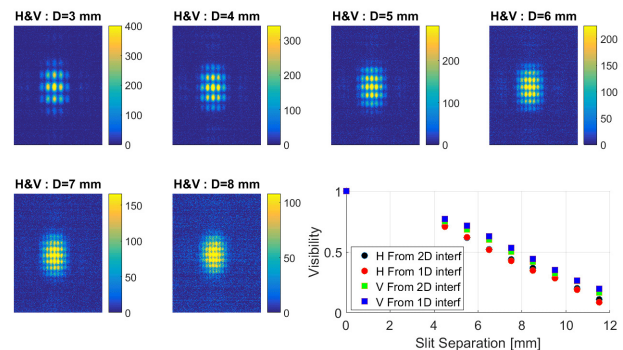


Figure 10: Interferograms recorded while scanning simultaneously the slit separation in the H and V plane. The visibilities from this 2D scan are compared to the ones obtained using separately the two assemblies.

obtained ($< 5\%$ discrepancy on beam size), shows that the coupling between the two planes is negligible and proves the feasibility of a 2D interferometer setup.

CONCLUSIONS

This paper covered the main aspects of the LHC interferometer design, implementation and commissioning. A comprehensive set of measurements were performed to compare the interferometer results to the standard imaging system at both the injection energy and 6.5 TeV. While good agreement was observed at injection energy, a scaling factor of about 1.3 is yet to be understood between the two systems at top energy. Nevertheless interferometry was able to provide coherent relative bunch size measurements at 6.5 TeV. The feasibility of 2S interferometric measurements has also been demonstrated.

REFERENCES

- [1] A.Fisher, "Expected Performance of the LHC Synchrotron-Light Telescope (BSRT) and Abort-Gap Monitor (BSRA)" PAC, SLAC-PUB-14098, 2010.
- [2] Goldblatt A, Bravin E, Roncarolo F, Trad G. "Design and Performance of the Upgraded LHC Synchrotron Light Monitor." Proc. of IBIC. 2013, Sep 1.
- [3] G. Trad, "Development and Optimisation of the SPS and LHC beam diagnostics based on Synchrotron Radiation monitors," Ph.D. thesis, Beams. Dept., CERN, 2015.
- [4] T. Mitsuhashi, "Beam Profile and Size Measurement by SR Interferometers", in Beam Measurement: Proceedings of the Joint US-CERN-Japan-Russia School on Particle Accelerators.
- [5] Trad G, Bravin E, Goldblatt A, Mazzoni S, Roncarolo F. "A novel approach to synchrotron radiation simulation". Proc. of IPAC, 2014.
- [6] Mitsuhashi, Toshiyuki, and Mikio Tadano, "Measurement of Wavefront Distortion Caused By Thermal Deformation Of Sr Extraction Mirror Based on Hartmann Screen Test And Its Application For Calibration Of SR Interferometer." PAC, 2001.
- [7] Trad, Georges, et al. "Performance of the upgraded synchrotron radiation diagnostics at the LHC." 7th International Particle Accelerator Conference (IPAC'16), Busan, Korea, May 8-13, 2016. JACOW, Geneva, Switzerland, 2016.
- [8] T. Mitsuhashi, private communication, August 2016.
- [9] T. Mitsuhashi, "Measurement of small transverse beam size using interferometry" Proc. of DIPAC 2001 – ESRF, Grenoble, France